Impacts of radiative corrections on measurements of lepton flavour universality in $B \to D\ell\nu_\ell$ decays

S. Klaver

INFN Laboratori Nazionali di Frascati, Via Enrico Fermi, 40, 00044 Frascati, Italy

Radiative corrections to $B \to D\ell\nu_\ell$ decays can have an impact on predictions and measurements of the lepton universality ratios $\mathcal{R}(D^+)$ and $\mathcal{R}(D^0)$. These proceedings summarise a study on the comparison between recent calculations of soft-photon corrections on these ratios and the corrections simulated by the PHOTOS package. Also the impact of Coulomb interactions, not simulated in PHOTOS, is discussed. Using pseudo-experiments, the effect of high-energy photon emission is studied in an LHCb-like environment, showing a bias of up to 7% on measurements of $\mathcal{R}(D)$.

I. INTRODUCTION

In the Standard Model (SM) it is assumed that the only difference between the three generations of leptons is their mass, and that their gauge couplings are the same. This assumption, called lepton universality (LU), can be tested by measuring the ratio of decay rates, which ensures that many experimental and theoretical uncertainties are cancelled in the ratio. One type of these LU measurements is performed using semileptonic B decays of the form $b \to c\ell^-\overline{\nu}_\ell$, commonly known as measurements of $\mathcal{R}(H_c)$. This is defined as

$$\mathcal{R}(H_c) = \frac{\mathcal{B}(H_b \to H_c\tau^-\overline{\nu}_\tau)}{\mathcal{B}(H_b \to H_c\ell^-\overline{\nu}_\ell)}, \qquad (1)$$

where H_b and H_c are a b and c hadron, respectively, and ℓ is either an electron or muon.

Measurements of $\mathcal{R}(H_c)$ have been performed by the LHCb, Belle and BaBar experiments. For $\mathcal{R}(D)$, the average of the measured value of $\mathcal{R}(D)$ is $0.349 \pm 0.027\,(\text{stat}) \pm 0.015\,(\text{syst})$ [1–3]. The predicted value for $\mathcal{R}(D)$, assuming isospin symmetry, is $\mathcal{R}(D) = \mathcal{R}(D^+) = \mathcal{R}(D^0) = 0.299 \pm 0.003$ [4–7]. Even though $\mathcal{R}(D)$ differs from the SM prediction by only 1.4σ, the deviation from the SM of the combined $\mathcal{R}(D)$ and $\mathcal{R}(D^*)$ is about 3.1σ [8].

Radiative corrections were long thought to be negligible at the level of precision of measurements and predictions of $\mathcal{R}(D)$. Recently, however, de Boer et al. [9] presented a new evaluation of the long-distance electromagnetic (QED) contributions to $\overline{B}^0 \to D^+\ell^-\overline{\nu}_\ell$ and $B^- \to D^0\ell^-\overline{\nu}_\ell$ decays, where $\ell^- = \mu^-, \tau^-$. These corrections are different for μ^- and τ^- decays, such that they do not cancel in $\mathcal{R}(D)$. A proper evaluation of the radiative corrections can alter SM predictions and increase their uncertainty.

In measurements of $\mathcal{R}(D)$, radiative corrections are simulated using the PHOTOS package [10, 11]. These proceedings, which are a summary of the studies described in Ref. [12], show the difference between the QED corrections simulated in PHOTOS and those predicted by Ref. [9]. They describe a study on the effects of under- or overestimating these corrections in simulation on measurements of $\mathcal{R}(D)$.

II. RADIATIVE CORRECTIONS IN PHOTOS

PHOTOS [10, 11] is a universal MC algorithm that simulates effects of QED corrections. The corrections simulated by PHOTOS have successfully been tested for W, Z, and B decays and should be tested for every type of measurements individually, especially when high precision is needed. Unlike Ref. [9], PHOTOS does not include Coulomb corrections. These corrections concern the enhancement of decay rates due to the interaction of two charged particles and are therefore relevant for the D^+ decay, but not for the D^0 decay.

Recent versions of PHOTOS include multi-photon emissions as well as interference between final-state photons, whereas Ref. [9] also includes the interference between initial- and final state photons. The calculation by de Boer et al. in Ref. [9] is valid in the regime in which the maximum energy of the radiated photons is smaller than the lepton mass, the muon mass in this case. PHOTOS also includes photon emission with higher energies. Neither Ref. [9] nor PHOTOS include the emission of photons depending on the hadronic structure. These so called structure-dependent photons impact the spin of the decay particle and may also interfere with bremsstrahlung photons.

To study the differences between Ref. [9] and PHOTOS, four samples ($\overline{B}^0 \to D^+\ell^-\overline{\nu}_\ell$ and $B^- \to D^0\ell^-\overline{\nu}_\ell$, where $\ell^- = \mu^-, \tau^-$) with three million B meson decays are generated by PYTHIA 8 [13, 14]. The B mesons decays are simulated by EVTGEN [15], including the QED corrections by PHOTOS v.3.56, with the "option with interference" switched on. For both the $B \to D\mu\bar\nu_\mu$ and $B \to D\tau\bar\nu_\tau$ decays considered, the HQET2 model is used with parameters from Ref. [8].

The four-momentum of the total radiated photons, p_γ, is defined as

$$p_\gamma = p_B - \left(p_D + p_{\ell^-} + p_{\overline{\nu}_\ell}\right), \qquad (2)$$

where p_B, p_D, $p_{\overline{\nu}_\ell}$, and p_{ℓ^-} are the four-momenta of the B, D, ℓ^- and $\overline{\nu}_\ell$, respectively. In agreement with Ref. [9], the radiation of the D decay products is not taken into account. The total energy of the radiated photons, E_γ, is computed in the B rest frame.

The variable E_{max} is defined as the maximum value
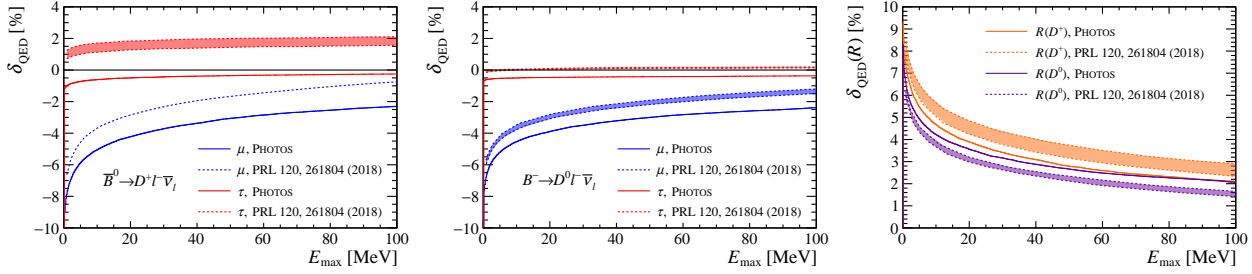
FIG. 1: Radiative corrections to the branching ratios of $\bar{B}^0 \to D^+\ell^-\bar{\nu}_\ell$ (left) and $B^- \to D^0\ell^-\bar{\nu}_\ell$ (middle) decays, as a function of $E_{\max}$. The long-distance QED corrections to $\mathcal{R}(D^+)$ (orange) and $\mathcal{R}(D^0)$ (violet) as a function of $E_{\max}$ (right). The plots are obtained from simulated data (solid lines) and from Ref. [9] (dashed lines).
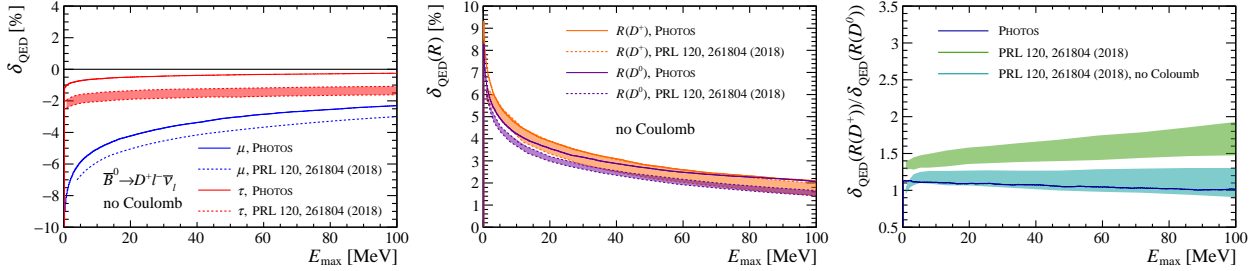

FIG. 2: Radiative corrections to the branching ratios of $\bar{B}^0 \to D^+\ell^-\bar{\nu}_\ell$ (left) and $\mathcal{R}(D^+)$ (middle) in the case that no Coulomb correction is applied. The plots are obtained from simulated data (solid lines) and from Ref. [9] (dashed lines). The plot on the right shows the ratio $\delta_{\mathrm{QED}}(\mathcal{R}(D^+))/\delta_{\mathrm{QED}}(\mathcal{R}(D^0))$.

that E_γ is allowed to have to consider $B \to D\ell\bar{\nu}_\ell(\gamma)$ signal rather than background. The QED correction, δ_{QED}, is given by the relative variation of the branching ratio when events with total radiated energy greater than $E_{\max}$ are discarded, calculated as

$$\delta_{\mathrm{QED}} = \frac{\int_0^{E_{\max}} N(E_\gamma)dE_\gamma}{\int_0^\infty N(E_\gamma)dE_\gamma} - 1 \,. \qquad (3)$$

Here, $N(E_\gamma)$ is the distribution of events with E_γ. The considered energy range is up to 100 MeV, covering the majority of radiative photons generated by PHOTOS.

Figure 1 shows comparisons between radiative corrections from PHOTOS and Ref. [9] to the $\bar{B}^0 \to D^+\ell^-\bar{\nu}_\ell$ (left) and $B^- \to D^0\ell^-\bar{\nu}_\ell$ (middle) branching ratios. These plots show differences of up to 2% for the $\bar{B}^0$ decays, and $0.5-1\%$ for B^- decays. This effect does not cancel even in the ratios of branching fractions. This is clearly visible in Fig. 1 (right), where radiative corrections on $\mathcal{R}(D)$, $\delta_{QED}(\mathcal{R})$, are shown as a function of $E_{\max}$. PHOTOS predicts a QED correction of 0.5% lower than Ref. [9] in $\mathcal{R}(D^+)$, and 0.5% higher in $\mathcal{R}(D^0)$.

A significant part of the radiative corrections in Ref. [9] originates from Coulomb interactions, which are not included in PHOTOS. Light leptons typically have a Coulomb correction of 1.023 [16], whereas the τ^- leptons in the $\bar{B}^0 \to D^+\tau^-\bar{\nu}_\tau$ decay have Coulomb corrections between 2.5% and 5.0%. The QED cor-

rections from PHOTOS for the D^+ decay mode are compared with predictions not including the Coulomb correction as provided by Ref. [9]. This reduces the difference of the corrections to the branching ratios between PHOTOS and the theoretical calculations to about 1% and brings the corrections on $\mathcal{R}(D^+)$ in close agreement, as is shown in Fig. 2.

Figure 2 (right) shows the ratio of QED corrections on $\mathcal{R}(D^+)$ over those on $\mathcal{R}(D^0)$. Both PHOTOS and the calculation in Ref. [9] without Coulomb corrections conserve isospin symmetry (δ_{QED} values for $\mathcal{R}(D^+)$ and $\mathcal{R}(D^0)$ agree within the errors), while Coulomb corrections introduce an isospin-breaking term.

III. EFFECTS ON LHCB-LIKE ANALYSIS

The comparison between Ref. [9] and PHOTOS can be made only for soft photons with energies up to 100 MeV. For higher energies, no calculations are available. However, PHOTOS generates also photons with higher energies in ranges where structure-dependent photons are relevant. These are used to study the effects of under- or overestimating radiative corrections in simulation for a measurement of $\mathcal{R}(D)$ in an LHCb-like environment.

A study is performed with the same data sets as described in the previous section by making a template fit to the $B \to D\mu^-\bar{\nu}_\mu$ and $B \to D\tau^-\bar{\nu}_\tau$ compo-
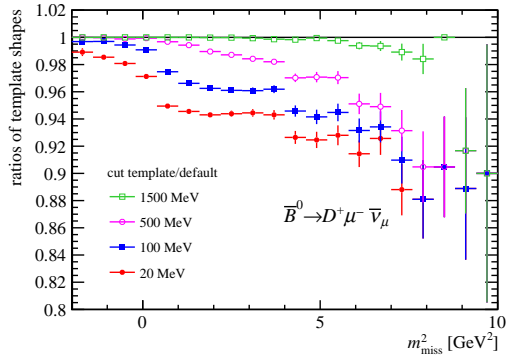
FIG. 3: Ratios of the cut $m_{\rm miss}^2$ distribution over the default $m_{\rm miss}^2$ distribution for the $\bar{B}^0 \to D^+ \ell^- \bar{\nu}_\ell$ decays, for the various cuts on $E_{\rm max}$ for the μ^- decay mode.

nents. This fit uses the same fit variables as LHCb's muonic $\mathcal{R}(D^*)$ analysis [17]. These are the muon energy computed in the B meson rest frame, E_μ; the missing mass squared, $m_{\rm miss}^2 = (p_B - p_D - p_\mu)^2$; and the squared four-momentum transferred to the lepton system, $q^2 = (p_B - p_D)^2$. Simulated data samples are created from a mixture of $B \to D\mu^-\bar{\nu}_\mu$ and $B \to D\tau^-\bar{\nu}_\tau$ decays, with radiative corrections generated by PHOTOS. Here $\mathcal{R}(D)$ is assumed to be 0.3 as predicted by the SM. No backgrounds are considered.

The fits are performed with templates that are created under the hypothesis that there is no radiation E_γ above $E_{\rm max}$. Five values of $E_{\rm max}$, 100, 300, 500, 800 and 1500 MeV, are chosen for this study. Fitting the templates to the simulated data sample with no cuts on radiation yields an estimate of the possible bias on $\mathcal{R}(D)$. This indicates the importance of simulating E_γ in the high-energy region. Note that LHCb analyses do not cut on radiative energy explicitly, but that implicitly applied cuts could alter this bias.

The acceptance of the LHCb detector is mimicked by applying selection requirements following Ref. [18]. The production and decay vertices are smeared to simulate the detector resolution and a cut on the flight distance is applied to resemble the trigger selection. At LHCb, the B meson momentum cannot be reconstructed due to the missing neutrino. Therefore, as in Ref. [17], the momentum of the B in the z direction, $(p_B)_z$, is approximated as $(p_B)_z = (m_B/m_{\rm vis})(p_{\rm vis})_z$, where m_B is the B mass, and $m_{\rm vis}$ and $(p_{\rm vis})_z$ are the mass and momentum in the beam direction of the visible decay products of the B meson, respectively.

The simulated sample size is based on an estimate of the yields for the Run II data-taking period using the reconstruction efficiencies from Ref. [17], the B production cross-section at 13 TeV, and branching fractions. This results in yields of data samples of 1.0×10^6 and 0.5×10^5 for the $\bar{B}^0 \to D^+ \ell^- \bar{\nu}_\ell$ decays, and 4.4×10^5 and 2.3×10^4 for the $B^- \to D^0 \ell^- \bar{\nu}_\ell$ decays, where the first yield represents the μ^- sample, and the second the τ^- sample.

The values of $\mathcal{R}(D)$ are determined from the fitted yields as well as the reconstruction efficiencies ε_μ and ε_τ for the μ^- and τ^- samples using

$$\mathcal{R}(D) = \frac{f_\tau}{1 - f_\tau} \frac{\varepsilon_\mu}{\varepsilon_\tau} . \qquad (4)$$

It is found that for this specific case study, the ratio of efficiencies is not affected by the cuts on E_γ. Combining the efficiencies with the fitted yields, the resulting values of $\mathcal{R}(D^+)$ as a function of the cut on $E_{\rm max}$ are shown in Fig. 4, which shows a dependence on $E_{\rm max}$. From here it is clear that there is a significant effect in underestimating the QED radiative corrections which could be up to 0.02 for both $\mathcal{R}(D^+)$ and $\mathcal{R}(D^0)$ values, corresponding to a relative bias of 7.5%. This is due to the change in template shapes when applying cuts on $E_{\rm max}$ which is most clearly visible in the $m_{\rm miss}^2$ distribution of the semimuonic decay, shown in Fig. 3. Since the template shapes of the semitauonic decays do not change significantly, this effect does not cancel in the ratio $\mathcal{R}(D^+)$.
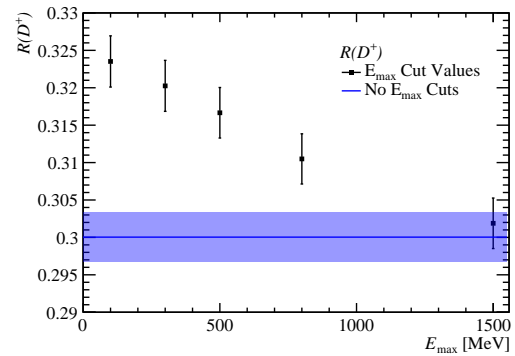

FIG. 4: Measured values of $\mathcal{R}(D^+)$ in a simplified LHCb-like analysis, as a function of $E_{\rm max}$. The blue band shows the fit result obtained with the same templates used to generate the pseudo-experiments.

The results for $\mathcal{R}(D^0)$ analysis look very similar to those for $\mathcal{R}(D^+)$ and are therefore omitted from these proceedings. In actual analyses, radiative corrections are present in data, and, at least partially, in simulation. Therefore this analysis is likely to be an overestimate on the bias.

Also the Coulomb correction impacts the shape of the fit templates and thus the experimental results of $\mathcal{R}(D^+)$. This bias is evaluated by weighting each event in the $\bar{B}^0 \to D^+ \ell^- \bar{\nu}_\ell$ decay by the Coulomb correction $\Omega_{\rm C}$. Changes in the q^2, $m_{\rm miss}^2$ and E_μ distributions are shown in Fig. 5. $\Omega_{\rm C}$ is mostly constant for the μ^- mode, but for the τ^- mode, a dependence on each of the three variables is shown. The above analysis is repeated while applying Coulomb corrections to the simulated data sample and not on the fit templates, resulting in a relative shift on $\mathcal{R}(D^+)$ of about -1.0%. No additional cuts on $E_{\rm max}$ are applied.
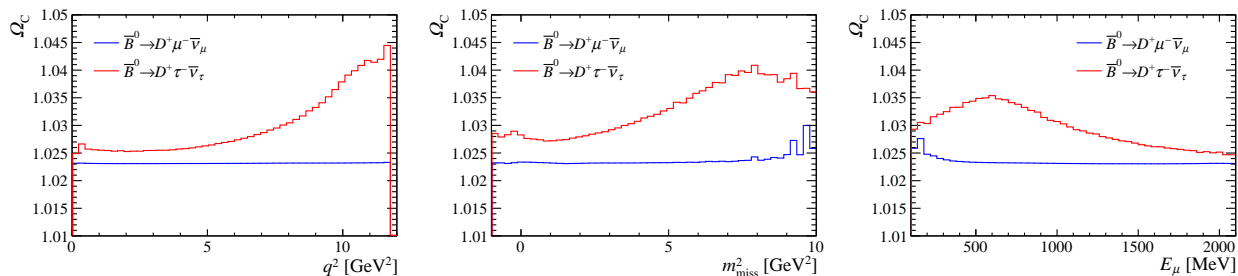
FIG. 5: Coulomb corrections as a function of q^2, m_{miss}^2, and E_μ for the $\overline{B}^0 \to D^+ \ell^- \overline{\nu}_\ell$ decays, where $\ell^- = \mu^-, \tau^-$.

IV.   CONCLUSIONS AND RECOMMENDATIONS

The QED corrections described in Ref. [9] are not fully included in the PHOTOS package which is used to simulate these corrections in analyses of the LHCb, Belle, and BaBar experiments. These different QED corrections affect the muonic and tauonic branching ratios at the level of a few percent. While calculating the ratios $\mathcal{R}(D)$, the differences largely cancel out when Coulomb corrections are ignored. Coulomb corrections are not present in PHOTOS and this results in a discrepancy between Ref. [9] and PHOTOS of up to 1 % on the ratio $\mathcal{R}(D^+)$.

Coulomb interactions mainly affect the kinematics of tauonic decays, changing the shape of the distributions used to determine their signal yields in an LHCb-like analysis. Not including these in simulated data can result in a bias of around 1% on measurements of $\mathcal{R}(D)$. Over- or underestimating radiative corrections can bias LHCb-like measurements up to 7%, resulting in a bias of 0.02 on $\mathcal{R}(D^+)$.

These studies must be repeated for each analysis individually because they are dependent on selection requirements as well as fit variables. For Belle II measurements, which have a better resolution on the kinematic variables [19] than LHCb, the effects could even be larger. Additional calculations of QED corrections on for $B \to D\ell\nu_\ell$ decays, specifically those involving high-energy and structure-dependent photons, are necessary in order to make measurements with higher precision.

Acknowledgments

[1] J. P. Lees et al. (BaBar), Phys. Rev. Lett. **109**, 101802 (2012), 1205.5442.

[2] M. Huschle et al. (Belle), Phys. Rev. **D92**, 072014 (2015), 1507.03233.

[3] A. Abdesselam et al. (Belle) (2019), 1904.08794.

[4] D. Bigi and P. Gambino, Phys. Rev. **D94**, 094008 (2016), 1606.08030.

[5] F. U. Bernlochner, Z. Ligeti, M. Papucci, and D. J. Robinson, Phys. Rev. **D95**, 115008 (2017), 1703.05330.

[6] S. Jaiswal, S. Nandi, and S. K. Patra, JHEP **12**, 060 (2017), 1707.09977.

[7] S. Aoki et al. (Flavour Lattice Averaging Group) (2019), 1902.08191.

[8] Y. Amhis et al. (Heavy Flavor Averaging Group), Eur. Phys. J. **C77**, 895 (2017), updated results and plots available at https://hflav.web.cern.ch, 1612.07233.

[9] S. de Boer, T. Kitahara, and I. Nisandzic, Phys. Rev. Lett. **120**, 261804 (2018), 1803.05881.

[10] P. Golonka and Z. Was, Eur. Phys. J. **C45**, 97 (2006), hep-ph/0506026.

[11] P. Golonka, Ph.D. thesis, Cracow, INP (2006), CERN-THESIS-2006-098.

[12] S. Calí, S. Klaver, M. Rotondo, and B. Sciascia (2019), 1905.02702.

[13] T. Sjöstrand, S. Mrenna, and P. Skands, JHEP **05**, 026 (2006), hep-ph/0603175.

[14] T. Sjöstrand, S. Mrenna, and P. Skands, Comput. Phys. Commun. **178**, 852 (2008), 0710.3820.

[15] D. J. Lange, Nucl. Instrum. Meth. **A462**, 152 (2001).

[16] D. Atwood and W. J. Marciano, Phys. Rev. **D41**, 1736 (1990).

[17] R. Aaij et al. (LHCb), Phys. Rev. Lett. **115**, 111803 (2015), [Erratum: Phys. Rev. Lett.115,no.15,159901(2015)], 1506.08614.

[18] G. Ciezarek, A. Lupato, M. Rotondo, and M. Vesterinen, JHEP **02**, 021 (2017), 1611.08522.

[19] W. Altmannshofer et al. (Belle-II) (2018), 1808.10567.